3D Printing of Metastructures for Passive Broadband Vibration Suppression

Conference Paper · July 2015

DOI: 10.13140/RG.2.1.5003.8489

3 authors, including:

Jared Hobeck
Kansas State University

Daniel Inman
University of Michigan

3D PRINTING OF METASTRUCTURES FOR PASSIVE BROADBAND VIBRATION SUPPRESSION

Jared D. Hobeck [1], Charles M.V. Laurent [2] and Daniel J. Inman [3]

[1] Department of Aerospace Engineering, The University of Michigan
1320 Beal Avenue, Ann Arbor, MI 48109-2140, USA
Email: jdhobeck@umich.edu, web page: http://www.umich.edu/

[2] Catholic Institute of Arts and Crafts
75 Avenue de Grande Bretagne, 31300, Toulouse, France
Email: charles.laurent@2015.icam.fr, web page: http://www.icam.fr/

[3] Department of Aerospace Engineering, The University of Michigan
1320 Beal Avenue, Ann Arbor, MI 48109-2140, USA
Email: daninman@umich.edu, web page: http://www.umich.edu/

Keywords: 3D Printed metastructures, Passive broadband vibration suppression

ABSTRACT

Metamaterial research began with a focus on modifying material properties in the molecular and nanometer scales such that desired physical characteristics including: thermal, optical, electrical, and wave propagation of the modified material outperformed those of the original. In this paper, a metastructure is a metamaterial inspired concept where unique combinations of material geometries and properties are integrated into a host structure on a centimeter to micrometer scale to achieve desired dynamic response characteristics. It will be shown that an array of small resonators can be built-in to a host structure and tuned by design to eliminate virtually all vibration within a desired frequency band. The proposed metastructure concept allows structural members to fulfill their overall mass, stiffness, strength, and geometric requirements while also acting as the vibration suppression system. This multifunctional structural design can potentially eliminate the need for conventional vibration suppression solutions that add excess material, mass, assembly time, and overall cost to achieve the same performance.

Continued advances in fabrication techniques, are allowing researchers and engineers to create structures with extremely complex geometries. Even material properties such as compliance and density can be varied throughout a single structure and interfaces can be created while the part is being printed. Here, the authors demonstrate how one can take advantage of 3D printing technologies to produce a metastructure prototype capable of broadband vibration suppression.

This paper includes a discussion of the metastructure design methodology along with both analytical and finite element modeling strategies. Experimental modal analysis results are presented and compared to those found using a commercially available finite element analysis code. Results show that axial vibration of a 3D-printed rod having only 10 internal resonators can be reduced over a frequency band of 275 Hz.

1 INTRODUCTION

Vibration suppression in aerospace structures, automobiles, and civil infrastructure is a multi-billion dollar industry. Unfortunately, most vibration suppression solutions are implemented after the structure is fabricated and require that mass be added to the structure. Another common vibration suppression method is adding viscoelastic material to the structure which again adds mass but also can have damping properties that are highly dependent on temperature which is of concern especially for aerospace applications. In addition to temperature sensitivity and/or excessive mass, another disadvantage of more traditional vibration suppression schemes is that they typically require assembly, installation, and possibly additional testing, all of which result in increased production time and cost.

The proposed passive vibration suppression solution takes advantage of uniquely designed structures called *metastructures* which are comprised of a distributed system of integrated internal oscillators. Each oscillator serves to absorb vibration from the entire structure or *host structure*. A single oscillator may have very little effect on the host structure; however, the collective dynamics of many oscillators has been shown to have significant vibration suppression capabilities.

Among the most recent investigations focused on vibration suppression with metastructures was performed by Zhu *et al.* (2014) where a uniquely designed array of chiral oscillators was shown to reduce vibration within a desired frequency band [1]. An earlier theoretical study proposed by Sun *et al.* (2010) focused on the modeling, analysis, and design of metamaterial beams for broadband absorption of vibration and acoustics [2]. A more applied study performed by Chen *et al.* (2011) investigated the dynamic effects of distributed arrays of local spring-mass resonators inserted in sandwich composite beams [3]. All of these and many other studies show that broadband vibration suppression can be attained by using arrays of local linear narrowband resonators. The literature also shows that a single resonator can have a large-amplitude broadband response simply by introducing a nonlinearity [4–6]. Hobeck and Inman (2015) introduced the concept of magnetoelastic metastructures for broadband vibration suppression where the nonlinear metastructure was shown to achieve 84.5% suppression compared to that of only 41% from an equivalent linear metastructure [7].

The research presented here demonstrates how one can take advantage of 3D printing technologies to produce a metastructure prototype capable of broadband vibration suppression. Continued advances in fabrication techniques, are allowing researchers and engineers to create structures with extremely complex geometries. Even material properties such as compliance and density can be varied throughout a single structure and interfaces can be created while the part is being printed. This paper includes a discussion of model-based design methodology for a 3D-printed metastructure along with both analytical and finite element modeling strategies. Experimental modal analysis results are presented and compared to those found using a commercially available finite element analysis code.

2 MODELING STRATEGIES

Both analytical and finite element modeling techniques were used to design the metastructure rod. The primary advantage of the proposed analytical model is that it can easily be implemented and executed in any computing software such as MATLAB with little computational effort. Because of this simplicity, the analytical model may be used for future optimization analyses. The finite element model was developed with ANSYS software, and was used as the primary design tool for the metastructure prototype discussed in the present study.

2.1 Analytical Modeling

There are two primary components of the analytical model. The first component is the absorber system which is composed of multiple resonators modeled as single degree of freedom (DOF) spring mass oscillators. For simplicity, all absorbers were assumed to be identical and evenly distributed along the rod. The second major analytical model component was the total rod absorber assembly which was modeled as a single DOF system using basic lumped parameter assumptions.

Each absorber was modeled as a cantilever beam with a large tip mass. Rayleigh's quotient was used to estimate the absorber natural frequency where the fundamental bending mode shape was assumed to be approximately equal to the cantilever under uniform gravitational loading with both shear and moment applied at the tip caused by the tip mass as illustrated in figure 1a.[1] After determining the mode shape estimate, the first natural frequency was found by calculating the ratio of potential to kinetic energy as,

[1] These beam deflection equations are readily available in most mechanics of materials textbooks.

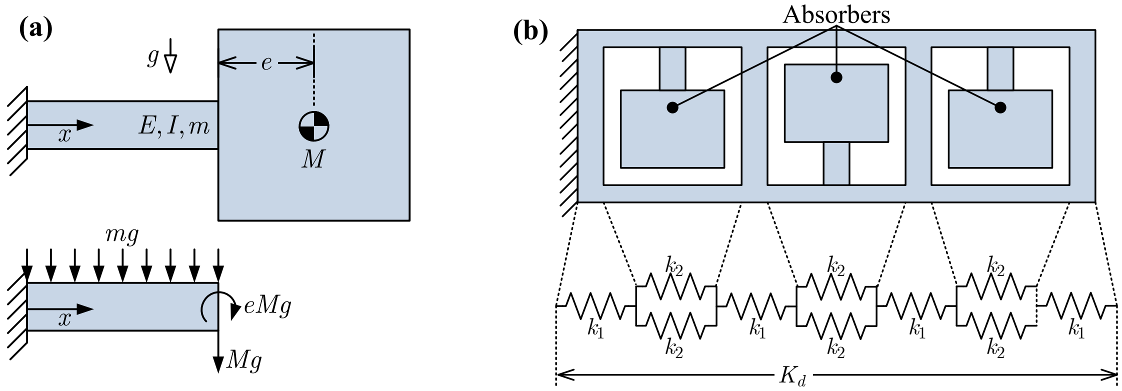

Figure 1: Schematics of (a) the absorber with applied loads used to estimate mode shape deflection and (b) a three absorber metastructure segment illustrating how the total stiffness was determined.

$$\omega_a^2 = \frac{\frac{1}{2}\int_0^L EI\left(\phi''\right)^2 dx}{\frac{1}{2}\int_0^L m\phi^2 dx + \frac{1}{2}M\left(\phi_L + e\phi_L'\right)^2 + \frac{1}{2}J\left(\phi_L'\right)^2} \tag{1}$$

where ω_a is the absorber natural frequency in rad/s, L is the absorber beam length, EI is the bending stiffness, ϕ is the estimated mode shape, x is the beam length coordinate, m is the linear mass density of the beam, M is the tip mass, e is the distance between the beam tip and the centroid of the tip mass, and J is the moment of inertia of the tip mass about the beam tip. Single or double primes denote first and second derivatives with respect to x respectively. A function with subscript L denotes that the function is evaluated at the beam tip, *i.e.* $\phi_L = \phi(x = L)$.

The lumped parameter model for axial vibration of the metastructure rod requires first defining the dynamic mass as,

$$M_d = \left(\frac{4}{\pi^2}\right)M_{tot} \tag{2}$$

where M_{tot} is the total mass of the rod absorber assembly and the mass ratio constant $4 / \pi^2$ is determined by equating the exact analytical expression for the first natural frequency of a fixed-free rod to that of a lumped mass approximation. This can be expressed as,

$$\frac{\pi}{2L}\sqrt{\frac{E}{\rho}} = \sqrt{\frac{K_{lm}}{M_{lm}}} = \sqrt{\frac{AE / L}{C\rho AL}} \tag{3}$$

where K_{lm} and M_{lm} are the axial lumped mass and stiffness of a uniform rod. Simplifying equation (3) and solving for the mass ratio C yields $C = 4 / \pi^2$. It is important to note that this mass ratio is only valid for rods with uniform mass and stiffness properties. Because this analysis is for identical and evenly spaced absorbers, it is assumed that the mass ratio in equation (2) is an appropriate approximation.

The lumped parameter stiffness of the rod is determined by considering that the rod can be represented as several linear springs connected in series. Each spring constant can be given as,

$$k_i = \frac{A_i E}{\ell_i} \tag{4}$$

where A is the axial cross-section area, E is the Young's modulus, ℓ is the segment length, and the subscript i denotes the i^{th} segment along the length of the rod. For this case, there are only two unique stiffness values as illustrated in figure 1b; therefore, the total axial stiffness can be given as,

$$K_d = \left(\frac{n+1}{k_1} + \frac{n}{2k_2}\right)^{-1} \tag{5}$$

where n is the number of absorbers, k_1 is the stiffness of the solid rod sections, and k_2 is the stiffness of the absorber sections as shown in figure 1b. Now that the lumped parameter mass and stiffness are defined, the natural frequency of the rod can be expressed as,

$$\omega_r = \sqrt{\frac{K_d}{M_d}} \tag{6}$$

where it is important to note that this is the estimated axial first natural frequency of the rod including the absorber mass but not including the dynamic effects of the absorber system. By designing the absorbers such that their natural frequency (equation (1)) is approximately equal to the natural frequency of the entire assembly (equation (6)) it is possible to eliminate or significantly reduce vibration at this design frequency ω_d where $\omega_d \approx \omega_a \approx \omega_r$.

2.2 Finite Element Modeling

In order to validate the analytical model and the general design approach, a finite element model was developed using ANSYS software. Similar to the analytical model, two primary components were considered – the absorbers and the total rod assembly. The goal was to design the absorbers to have approximately the same natural frequency as the first natural frequency of the rod assembly. Unlike with the analytical model, the finite element model required that this frequency matching be done iteratively. Since approximate dimensions could quickly be determined from the analytical model, these were the starting dimensions for the finite element model design and the frequencies converged after only a few iterations.

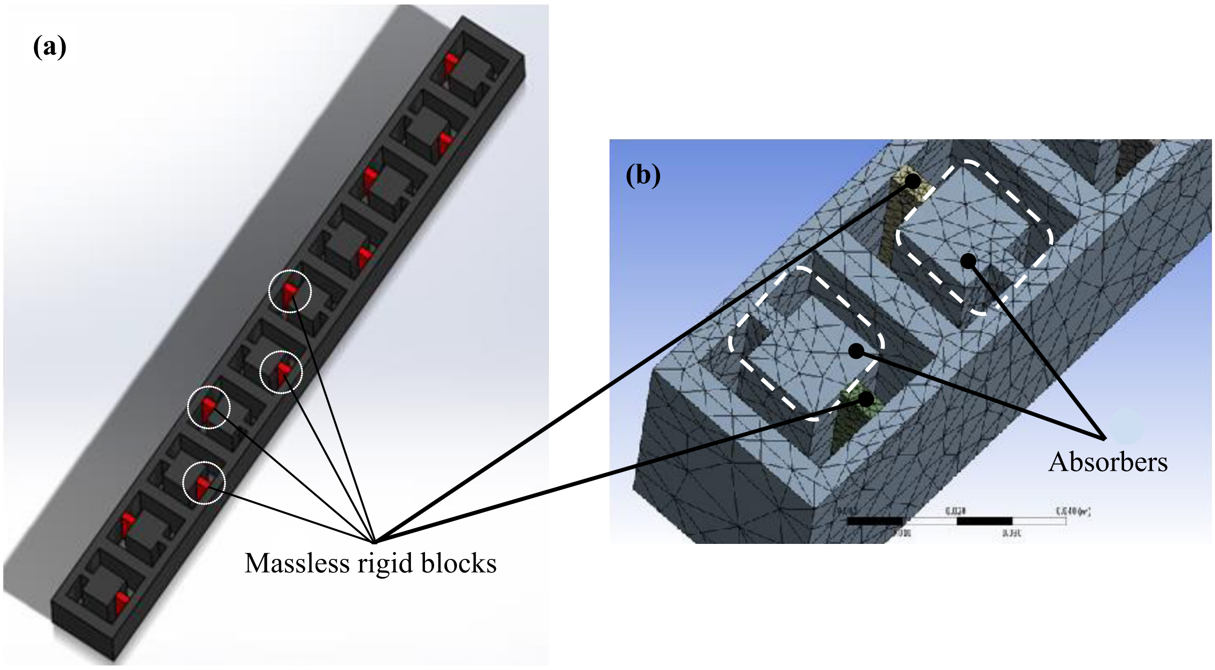

Figure 2: Views of the 3D model developed for finite element analysis showing the absorber blockers for (a) the full view of the ten absorber model and (b) a more detailed view including the mesh.

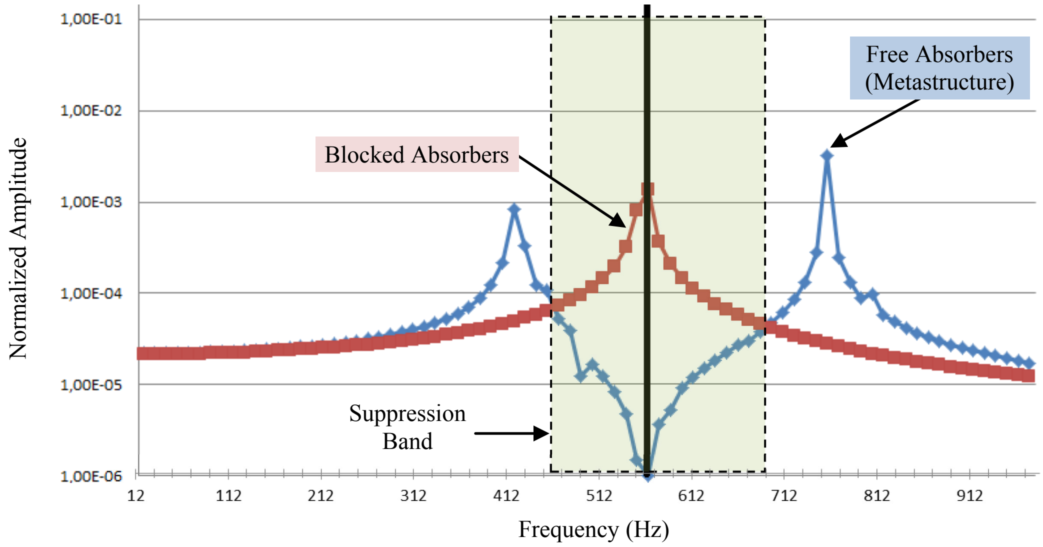

Figure 3: Summary of finite element modal analysis results showing that vibration at the design frequency of 563 Hz is suppressed.

Recall that the analytical model considered the absorber mass but not the absorber dynamics. This condition will be referred to as *blocked* while the case where the absorber dynamics are included will be referred to as the *free* condition. These two conditions were considered so that the effect of the absorber system on the frequency response was attributed only to the absorber dynamics thus eliminating mass loading effects. The blocked absorber condition was simulated by attaching the free end of each absorber to the sidewall of the rod with a small block of material as shown in figure 2. This block material had a density orders of magnitude less than, and a Young's modulus orders of magnitude more than the absorber and rod material.

After matching the first natural frequency of the absorber (bending) to that of the total rod assembly (axial) for the blocked absorber condition, modal analysis was performed on the rod for both the blocked and free absorber conditions. Figure 3 summarizes these modal analysis results showing frequency response plots of the normalized tip amplitude as a function of excitation frequency for axial vibration of the fixed-free rod assembly. Results in figure 3 clearly demonstrate that the free absorber (metastructure) system virtually eliminates vibration at the design frequency of 563 Hz.

3 EXPERIMENTAL ANALYSIS

Finite element analysis results shown in the previous section identified a final metastructure design which was shown to significantly reduce vibration at or near the first axial natural frequency. A prototype of this final design was fabricated by 3D Systems Inc. using a standard 3D printing technique called stereolithography. A series of simple experiments were performed on the 3D-printed metastructure prototype for proof-of-concept, model updating, and model validation purposes. This section discusses details and summarizes results of these experiments.

3.1 Setup, Strategy & Procedure

Recall from section 2.2 that both *free* and *blocked* absorber conditions were considered primarily for design purposes, but also to demonstrate the effect of the absorber system without significantly modifying the total mass of the structure. The prototype was printed in the free absorber condition, *i.e.* the absorbers were unconstrained and free to vibrate at their designed frequency. While adding rigid massless blocks was simple to implement in the analytical and finite element models, achieving a perfect blocked absorber condition during experimentation was not possible. In order to approximate this blocked condition, small slender pieces of foam core sandwich material were pressed between the free end of the mass and the metastructure wall as shown in figure 4a.

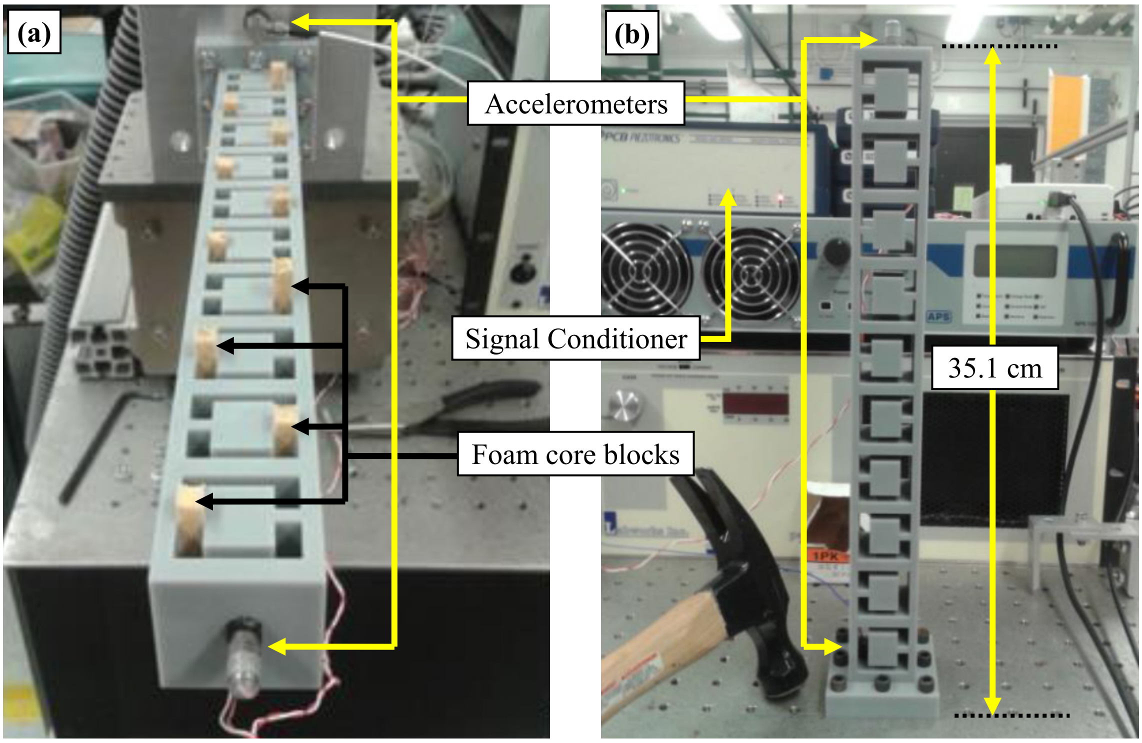

Figure 4: Snapshots of the 3D-printed metastructure prototype with both a) blocked and b) free absorber conditions used for the validation experiments.

These small inserts added negligible amounts of mass to the total structure while constraining relative motion of the absorber masses, thus rendering the absorber system useless.

Accelerometers were attached to the metastructure prototype – one to the fixed base and one to the free end as shown in figure 4. Measurements from these accelerometers were used to compute the frequency response of the free end relative to the base. The structure was excited with an impulse by using a hammer to strike the fixed base as shown in figure 4b for both free and blocked absorber conditions (free absorber condition shown). This impulse base excitation technique was found to produce higher quality measurements compared to those from sine sweep base excitation from an electrodynamic shaker.

3.2 Summary of Results

Results of the free and blocked impulse excitation measurements are compared in figure 5 where the effect of the absorber system is clearly seen. As expected for the blocked case where the absorber system is constrained, there is an obvious single resonant peak at approximately 671 Hz, the first axial natural frequency of the structure. When the foam core blocks are removed, the absorber system reduces or completely eliminates vibration at and around the design frequency of 671 Hz which is similar to that seen for the finite element model in figure 3. Not only was the first axial mode vibration suppressed, but vibration amplitude of the metastructure was less than that of the blocked condition from 550 Hz to 825 Hz – a band of 275 Hz. Results in figure 5 also show that the global vibration amplitude was reduced for the free absorber case.

The first axial natural frequency of the blocked absorber case predicted by the analytical and finite element models was approximately 597 Hz and 563 Hz respectively which was significantly less than that observed in experiment (671 Hz). This disparity was assumed to be caused by not having exact knowledge of the mass density and Young's modulus of the printed prototype. This assumption was validated by using the maximum and minimum material property values as published on the manufacturer's website in the finite element model to determine if the experimental results occurred within the range of possible solutions.

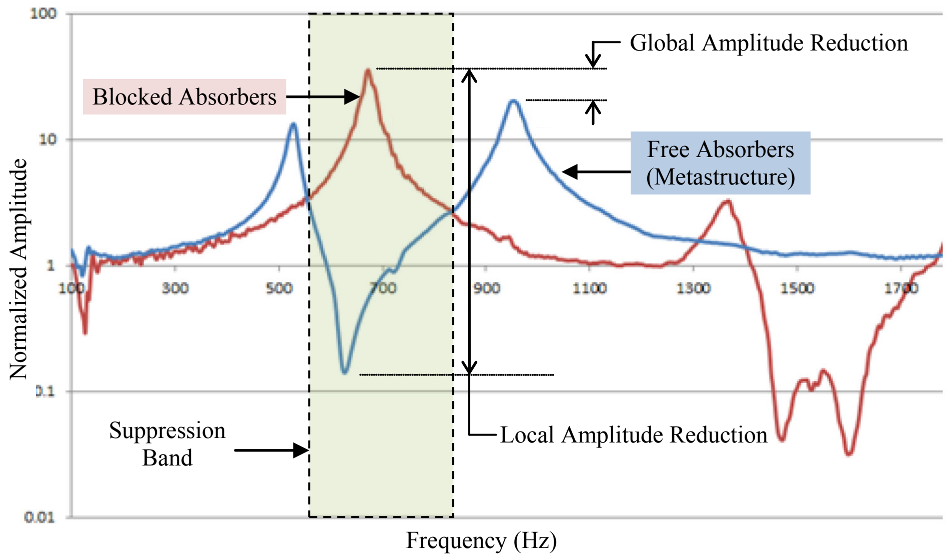

Figure 5: Frequency response measurements of the metastructure prototype comparing the free and blocked absorber cases.

	Finite Element (Hz)	Analytical (Hz)	Experiment (Hz)
Absorbers	563	579	626
Rod (Blocked Absorbers)	563	597	671

Table 1: First natural frequencies of a single absorber (bending) and the total rod (axial) with the blocked absorber condition comparing the analytical and experimental results to the finite element model design.

These modeling results showed that the first natural frequency had a possible range of 570 Hz to 680 Hz which includes the observed natural frequency of 671 Hz thus validating the analytical and finite element modeling approach.

Table 1 provides a final summary of results from both analytical and finite element models along with the experimental results. This summary of results lists the first natural frequency of the absorbers (bending) and the first natural frequency of the total rod assembly (axial) for the blocked absorber condition. Ideally, these two frequencies should be equal as they were designed to be for the finite element model. The analytical model results in table 1 were found using the model proposed in section 2.1 with the exact geometry and material properties used in the finite element model. As one should expect, the reduced order analytical model overestimated the higher fidelity finite element model but by a maximum error of only 6%. The experimental results initially deviated significantly from those of both models; however, as was previously discussed, the models agreed very well with experiments after updating the material properties to within the range of published values.

4 CONCLUDING STATEMENTS

The research presented here highlights initial modeling and experimental results of an investigation focused on passive vibration suppression using 3D-printed metastructures. Both analytical and finite element modeling methods were presented and successfully applied to the proposed axial vibration metastructure prototype design. A 35.1 cm long, ten absorber, metastructure prototype was fabricated based on the finite element model-driven design using a standard commercially available 3D printing technique called stereolithography. Experimental results presented in this paper were shown to agree well with model predictions. It was shown that natural frequencies calculated using the proposed lumped parameter analytical model overestimated those predicted with the finite element model, but only by a maximum of 6%. The measured and predicted frequency response of the metastructure prototype was shown to virtually eliminate vibration at the desired design frequency while suppressing vibration over a frequency band of up to 275 Hz.

Results of this research show that 3D-printed metastructures can be quite effective at vibration suppression even with fairly simple geometries. Therefore, immediate future work should focus on exploring the vast metastructure design space made possible by existing 3D printing technology.

ACKNOWLEDGEMENTS

This research is supported in part by the United States Air Force Office of Scientific Research under grant number: FA9550-14-1-0246, "*Electronic Damping in Multifunctional Material Systems*" monitored by Dr. BL Lee.

REFERENCES

[1] Zhu, R., Liu, X.N., Hu, G.K., Sun, C.T., and Huang, G.L., "A chiral elastic metamaterial beam for broadband vibration suppression," *Journal of Sound and Vibration* **333**(10), 2759–2773 (2014).

[2] Sun, H., Du, X., and Pai, P.F., "Theory of metamaterial beams for broadband vibration absorption," *Journal of Intelligent Material Systems and Structures* **21**(11), 1085–1101 (2010).

[3] Chen, J.S., Sharma, B., and Sun, C.T., "Dynamic behaviour of sandwich structure containing spring-mass resonators," *Composite Structures* **93**(8), 2120–2125 (2011).

[4] Karami, M.A., and Inman, D.J., "Linear and nonlinear energy harvesters for powering pacemakers from heart beat vibrations," *Proceedings of SPIE - The International Society for Optical Engineering* **7977**, San Diego, CA (2011).

[5] Arrieta, A.F., Hagedorn, P., Erturk, A., and Inman, D.J., "A piezoelectric bistable plate for nonlinear broadband energy harvesting," *Applied Physics Letters* **97**(10) (2010).

[6] Erturk, A., Hoffmann, J., and Inman, D.J., "A piezomagnetoelastic structure for broadband vibration energy harvesting," *Applied Physics Letters* **94**(25) (2009).

[7] Hobeck, J.D., and Inman, D.J., " Magnetoelastic metastructures for passive broadband vibration suppression ," *Proceedings of SPIE - The International Society for Optical Engineering* **9431**, 943119–9 (2015).